PNAS RESEARCH ARTICLE | EVOLUTION

Experimental evolution reveals the synergistic genomic mechanisms of adaptation to ocean warming and acidification in a marine copepod

Reid S. Brennan[a,b,c,1], James A. deMayo[d], Hans G. Dam[d], Michael Finiguerra[e], Hannes Baumann[d], Vince Buffalo[f], and Melissa H. Pespeni[a,1]

Edited by Stephen Palumbi, Department of Biological Sciences, Stanford University, Pacific Grove, CA; received January 27, 2022; accepted August 8, 2022

Metazoan adaptation to global change relies on selection of standing genetic variation. Determining the extent to which this variation exists in natural populations, particularly for responses to simultaneous stressors, is essential to make accurate predictions for persistence in future conditions. Here, we identified the genetic variation enabling the copepod *Acartia tonsa* to adapt to experimental ocean warming, acidification, and combined ocean warming and acidification (OWA) over 25 generations of continual selection. Replicate populations showed a consistent polygenic response to each condition, targeting an array of adaptive mechanisms including cellular homeostasis, development, and stress response. We used a genome-wide covariance approach to partition the allelic changes into three categories: selection, drift and replicate-specific selection, and laboratory adaptation responses. The majority of allele frequency change in warming (57%) and OWA (63%) was driven by shared selection pressures across replicates, but this effect was weaker under acidification alone (20%). OWA and warming shared 37% of their response to selection but OWA and acidification shared just 1%, indicating that warming is the dominant driver of selection in OWA. Despite the dominance of warming, the interaction with acidification was still critical as the OWA selection response was highly synergistic with 47% of the allelic selection response unique from either individual treatment. These results disentangle how genomic targets of selection differ between single and multiple stressors and demonstrate the complexity that nonadditive multiple stressors will contribute to predictions of adaptation to complex environmental shifts caused by global change.

evolve and resequence | zooplankton evolution | global change adaptation

Human activity is driving dramatic environmental changes across the globe, and understanding how adaptation will proceed under this rapid change is a crucial challenge. After rapid environmental shifts, populations may go extinct unless they evolve. Selection due to environmental shifts can act on standing genetic variation within a population (1), resulting in rapid phenotypic (2, 3) and genomic changes (4–6). To effectively manage species and predict their ability to tolerate environmental change, it is necessary to understand the potential for and mechanisms of adaptation prior to the changes occurring in the wild.

Evolve-and-resequence (E&R) approaches are ideal for addressing this problem, because populations can be reared under predicted future environments and allele frequencies quantified at multiple time points to directly observe evolutionary potential and the mechanisms of adaptation (7, 8). This method is powerful in that it reveals both the presence of standing adaptive genetic variation and the mechanistic basis of adaptation at the genetic level. However, revealing the effects of selection on allele frequency changes remains a challenge for E&R studies (9), particularly when adaptation proceeds from standing genetic variation on polygenic traits, those likely to be under selection during global change (10). Adaptation from standing variation associated with polygenic traits can lead to diffuse and subtle signals of selection that can be difficult to distinguish from drift (11, 12). In addition, incorporating appropriate experimental controls is essential to prevent spurious results from phenomena such as adaptation to laboratory conditions, drift, or nonparallel responses to selection (13, 14). New covariance-based methods improve the power of identifying responses to selection using replicated genomic samples through time (14, 15) and can be extended to control for laboratory adaptation. However, no work yet has leveraged these covariance-based methods to understand rapid evolutionary responses to global change conditions.

Significance

Resilience to global change will require adaptation to multiple concurrent environmental changes. However, it is unclear if adaptations to multiple stressors can be predicted from the sum of single-stressor adaptation. To answer this question, we experimentally evolved a marine copepod to warming, acidification, and their combination, finding that copepods were able to adapt to all conditions over 25 generations. Warming was a much stronger selective pressure than acidification alone and under multiple-stressor conditions. Nevertheless, the multiple-stressor response to selection was synergistic and unique from either single stressor. Thus, adaptation to single stressors may not reveal adaptive potential or mechanisms of adaptation under multiple stressors, demonstrating the complexity of predicting adaptive responses under multifaceted environmental change.

The authors declare no competing interest.

This article is a PNAS Direct Submission.

Author contributions: R.S.B., J.A.d., H.G.D., M.F., H.B., and M.H.P. conceptualized and designed research; J.A.d. performed research; R.S.B., J.A.d., and V.B. performed data collection and analysis; R.S.B. and M.H.P. wrote the paper; and R.S.B., J.A.d., H.G.D., M.F., H.B., V.B., and M.H.P. reviewed and edited the paper.

See online for related content such as Commentaries.

[1]To whom correspondence may be addressed. Email: rbrennan@geomar.de or mpespeni@uvm.edu.

This article contains supporting information online at http://www.pnas.org/lookup/suppl/doi:10.1073/pnas.2201521119/-/DCSupplemental.

Published September 12, 2022.

The world's oceans are particularly vulnerable to human activity as unprecedented increases in atmospheric CO_2 lead not only to higher global temperatures but also decrease ocean pH due to CO_2 dissolution, a phenomenon known as ocean acidification (16, 17). These environmental changes could fundamentally alter marine ecosystems, particularly if they affect zooplankton that link primary producers with higher-level consumers and are essential in ocean biogeochemical cycles (18–20). For zooplankton, pH declines may increase the cost of acid–base regulation (21) while temperature exposure beyond an organism's optimum drives quick performance declines (22). As such, there has been considerable effort to understand how zooplankton will be able to evolve in response to shifting global conditions (23–29). However, a limitation of previous work measuring evolutionary potential has been the focus on single stressor–selective pressures. Given the simultaneous shift in abiotic factors occurring under climate change, it is essential to understand the combined effects of multiple stressors (30). This is especially important as multiple stressors can have additive, antagonistic, or synergistic effects (31), and studying stressors both alone and in combination will reveal the physiological and evolutionary processes that promote resilience.

Acartia tonsa is one of the most abundant copepods globally and a dominant species in coastal ecosystems where it is the primary food source of numerous fishes (32). Given this, the resilience of *A. tonsa* is essential in preserving ecosystem functioning under global change. We previously conducted a selection experiment where we reared *A. tonsa* for 25 generations (~1 y) to characterize fitness-related trait responses to warming, acidification, and their combination (OWA) (33). We found that exposure to OWA conditions drove a decrease in population fitness that largely recovered by three generations through improved egg-hatching success and earlier reproductive timing. However, fitness measurements at later generations revealed incomplete adaptation of *A. tonsa* to OWA selection. In contrast, warming and acidification alone had minor effects on population fitness. These results suggest that the interaction of the two stressors in OWA conditions may have complex, nonadditive effects.

Here, we used the same populations from our evolution experiment to measure genomic responses to 25 generations of selection in ambient, warming, acidification, and OWA conditions. We specifically asked: 1) What is the contribution of selection to evolutionary change? 2) To what degree are adaptive changes shared between the single and multiple stressors? 3) What are the genes and functional mechanisms underlying rapid adaptation to warming, acidification, and OWA conditions? We demonstrate that *A. tonsa* has sufficient adaptive genetic variation to evolve in response to warming, acidification, and OWA conditions, show the large effects of warming on copepod adaptation relative to acidification, and reveal the synergistic effects of warming and acidification when combined as a multiple stressor. Finally, these results reveal the importance of controlling for laboratory adaptation in E&R experiments. As E&R experiments continue to expand into nonmodel systems (34), our results demonstrate the utility of this method and the need to incorporate multiple stressors which are relevant to diverse ecosystems. This approach will assist in understanding mechanisms of adaptation to future environmental conditions for organisms across ecosystems.

Results

Genome-Wide Variation in Response to Experimental Selection. To quantify genomic response to selection of *A. tonsa*, samples were collected from each of four replicates of acidification, warming, and OWA treatments at generation 25 and from an ambient control at generations 0 and 25. We designed 32,413 capture probes to target both regulatory (11,102) and coding (21,311) regions of the genome and used pooled-capture sequencing of 50 individuals per replicate to characterize the allele frequency changes across the experiment. After filtering variants, we obtained 394,667 single-nucleotide polymorphisms (SNPs) with no missing data across all samples. The founding population possessed high genome-wide genetic diversity on which selection could act (Tajima's π: 0.0148 ± 0.0004). Principal-component analysis (PCA; Fig. 1) showed that the variance in genome-wide allele frequencies for all samples clustered by treatment group, and F25 samples had diverged from the F0 founding population along PC1 (15.82% of the variation). There was also separation of the warming and OWA treatments from ambient and acidification treatments along this axis. PC2 (10.99% of the variation) further separated each treatment group into distinct clusters.

Identifying the Specific Targets of Selection. To identify the genetic variation responding to selection consistently across all replicates within a treatment, we simulated the degree of drift expected with our experimental design across 25 generations (*Methods*) and used these simulations with Cochran–Mantel–Haenszel (CMH) tests to identify loci that were evolving more than we would expect by drift alone. Accordingly, we found 7,926 (2.0% of all SNPs), 6,270 (1.59%), and 1,713 (0.4%) SNPs that were candidate targets of selection for OWA, warming, and acidification, respectively (Fig. 2 and *SI Appendix*, Fig. S1). The movement of the ambient lines in principal-component space relative to the founding population replicates (Fig. 1) suggested the presence of adaptation to ambient conditions and the CMH tests supported this with evidence for adaptation of 3,150 candidate SNPs (0.8% of total SNPs).

Responses to selection were both unique and shared within and between treatments. OWA showed the largest unique response to selection with 4,261 loci (54% of OWA significant loci) as compared with 2,365 (38%) in warming, 302 (18%) in acidification, and 1,370 (43%) in ambient. Pairwise shared response between treatment groups was greater than by random chance for all groups (exact test, $P < 0.0001$). This shared response was highest between warming and OWA (3,475 SNPs; 24% of total significant SNPs between both treatments) and much lower for OWA and acidification (1,124 SNPs;

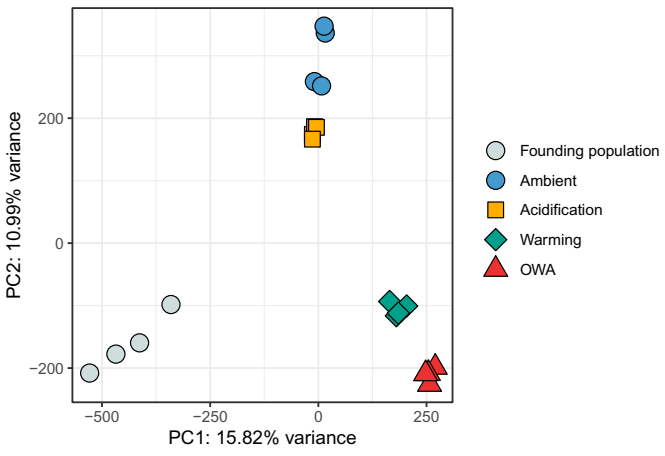

Fig. 1. PCA of allele frequencies from 394,667 SNPs across the genome where color and shape distinguish treatment groups. The founding population is F0; all others are from F25.

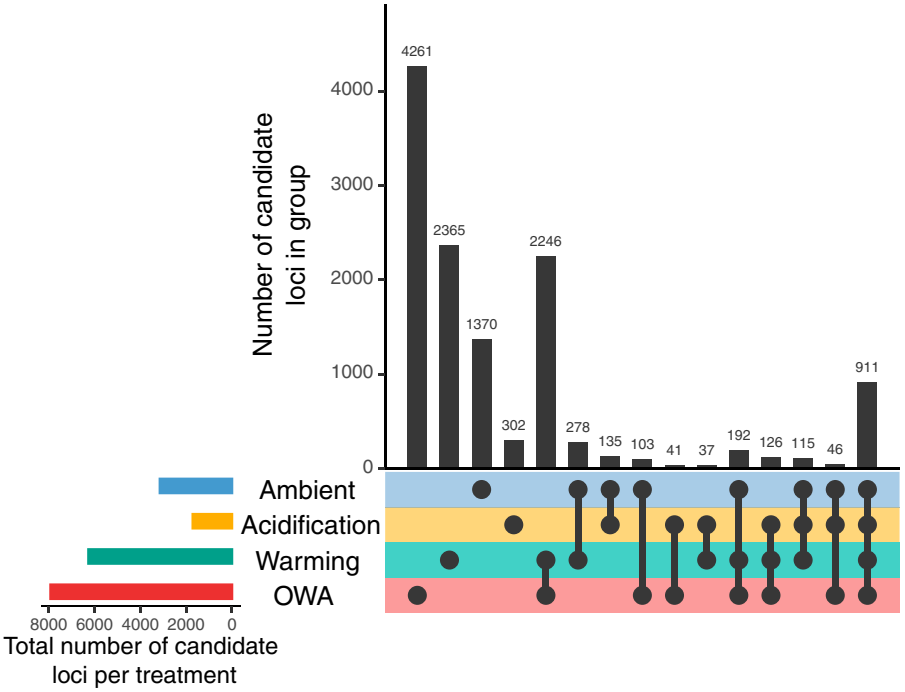

Fig. 2. Candidate SNPs exceeding drift expectations identified from Wright–Fisher simulations. The horizontal bars indicate the total number of candidate loci in each group while the vertical bars show the number in each category. Black points show treatments in a category where multiple groups are indicated by connected lines. Note that the counts in each group are exclusive; for example, the number of loci in the OWA-alone category are those loci not shared with any other group.

12%) and acidification and warming (1,189 SNPs; 15%). While there was limited overlap in the response between any three treatments, there was a large shared response between all groups (911 SNPs), suggesting a strong signal of shared adaptation to laboratory conditions. To understand the response to each selection regime independent of laboratory conditions, we removed the shared signal of laboratory adaptation and found that 21% (2,372 SNPs) of the response between OWA and warming was still shared as compared with 2.3% (167 SNPs) between OWA and acidification and 3.1% (163 SNPs) between acidification and warming.

To further characterize the genomic regions responsive to selection, we tested for overrepresentation of candidate loci in coding, promoter, intron, downstream, and unannotated regions. The candidate loci were unequally distributed across the genome and were overrepresented in coding regions for OWA (5,198 OWA candidate loci in coding regions/7,926 all OWA candidate loci = 0.656) and warming treatments (4,049/6,270 = 0.646) relative to genome-wide patterns (229,898 loci in coding regions/394,667 all loci = 0.583) (*SI Appendix*, Table S1; χ^2 test, $P < 0.001$). Acidification had fewer candidate loci in coding regions (885/1,713 = 0.517; $P = 0.009$) and ambient lines followed genome-wide expectations (1,778/3,150 = 0.564; $P = 0.73$). For OWA and warming but not ambient and acidification there were fewer candidate loci on scaffolds with no gene annotations ($P < 0.001$; genome-wide: 54,228/394,667 = 0.137; OWA: 702/7,926 = 0.089; warming: 577/6,270 = 0.092; acidification: 278/1,713 = 0.162; ambient: 431/3,150 = 0.134). These regions with no annotation are likely in regions that are poorly assembled or those that lack protein-coding regions. This inflation of selection in coding regions of genes for OWA and warming suggests that selection was disproportionately targeting protein-coding variation during the adaptation process.

Tests for gene ontology (GO) functional enrichment were used to gain insight into the mechanisms that may underlie adaptation to the different conditions. We tested for enrichment within the candidate SNPs for all groups of treatments presented in Fig. 2 (*SI Appendix*, Fig. S2 and Table S2). We found significant enrichment for all loci uniquely responding to single treatments though the number of terms was much higher for OWA (32 significant GO terms) and warming (47 significant GO terms) as compared with ambient (18 GO terms) and acidification 14 GO terms. Pairwise overlapping SNPs showed limited enrichment with the exception of OWA and warming (39 GO terms). Finally, loci responding across all selection regimes were enriched for four GO terms. For OWA, enriched categories were related to developmental, ion homeostasis, and NADP biosynthetic processes (*SI Appendix*, Table S2). Categories enriched among loci responding to warming were largely related to development, while categories enriched among loci responding to acidification included ion transport, methylation, and regulation of reactive oxygen species. Categories enriched among loci responding to ambient laboratory conditions included several related to the regulation of mitotic processes. Lastly, categories enriched among loci responding to both OWA and warming (39 significant GO terms) were largely related to development, lipid metabolism, actin, cytoskeletal, and microtubule processes, and regulation of messenger RNA stability and transcription.

Contribution of Selection, Drift and Replicate-Specific Responses, and Laboratory Adaptation to Allele Frequency Change. Leveraging both the replicated and temporal nature of our experimental design, we used the temporal covariance-based method cvtk (14) to identify even subtle contributions of polygenic selection to genome-wide allele frequency change. In contrast to other methods, such as CMH, that look for relatively strong selection at a few loci, temporal covariance-based methods quantify how much of allele frequency change across replicates is due to shared selection pressures rather than random genetic drift or replicate-specific responses.

We calculated pairwise covariances in allele frequency change from F0 to F25 in 10,000-bp windows between all pairwise replicates (*SI Appendix*, Fig. S3). From this, we determined the convergent correlation, a standardized measure of how similar allele frequency changes are between replicates within or between different treatments due to a convergent selection response (Fig. 3*A*). A high convergent correlation indicates parallel changes in allele frequency due to a shared response to a selective pressure. In contrast, under drift or replicate-specific selection responses, allele frequency changes would be independent across replicates, leading to a convergent correlation of zero. We observed the highest convergent correlations between the four replicates within each selection regime, indicative of parallel responses to selection pressure and providing evidence that the selection regimes are acting consistently across replicates within a treatment (Fig. 3A). By contrast, comparisons between replicates across treatment groups generally had weaker convergent correlations than the within-treatment comparisons (Fig. 3*A*; see *SI Appendix*, Fig. S4 for 95% block-bootstrapped CIs). The exception to this was between OWA and warming treatments where the intertreatment convergent correlations approached or exceeded within-treatment comparisons (Fig. 3*A*). This high similarity in response to selection between OWA and warming indicates shared targets of selection between the two conditions; this pattern was not present between other intertreatment comparisons.

The contribution of selection to the total variance in allele frequency change was quantified as the ratio of the average shared pairwise covariances across replicates to total variance (Fig. 3*B*). The OWA line was most strongly affected by selection with 67.6% (CI[66.9, 68.3]) of the total variance in allele frequency change due to selection. Warming was slightly, but significantly, lower (65.2% CI[64.3, 66.2]) than OWA, and acidification showed the lowest percentage of variance due to selection at 33.7% (CI[32.2, 35.3]).

Estimates of shared variance between samples could be inflated due to the shared variance driven by laboratory selection (*SI Appendix*, Figs. S3 and S4). Because the ambient and any treatment line shared only the laboratory environment but not the selective pressure of interest, the covariance between ambient and a selected line represented adaptation to the laboratory environment and could therefore be estimated and accounted for. The total estimated laboratory effects were lower in OWA conditions (0.0024, 95% CI[0.0018, 0.0029]) than either warming (0.0036, CI[0.0030, 0.0041]) or acidification (0.0033, CI[0.0029, 0.0038]). After accounting for the laboratory adaptation signal, the percent of total allele frequency change variance due to selection decreased for all treatments, but the rank order and significance remained: OWA 63.2% CI[62.1, 64.2], warming 56.5% CI[55.1, 57.9], and acidification 20.1% CI[18.5, 21.7] (Fig. 3*B*).

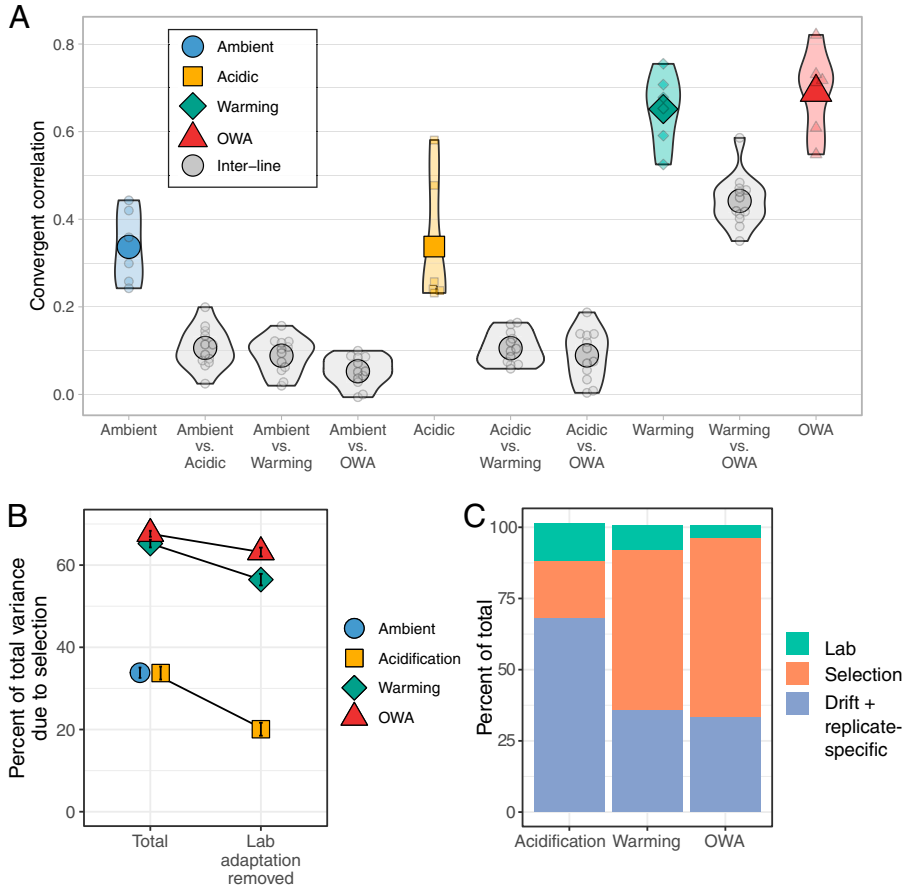

Fig. 3. (*A*) Convergent correlations of allele frequency change from F0 to F25. Higher values indicate a more similar change in allele frequency between two samples. Each small point is the convergent correlation between two samples and the large points are the mean of each group comparison. For visual clarity, we omit the CIs of each pairwise convergent correlation; see *SI Appendix*, Fig. S4 for these values. (*B*) Percent of total variance in allele frequency due to selection with and without accounting for laboratory adaptation. Lab adaptation was removed by quantifying the shared response between the ambient and each treatment group. Error bars are 95% bootstrapped CIs. (*C*) The contribution of laboratory selection, treatment selection, and drift plus replicate-specific responses to the total variance of allele frequency change from F0 to F25. The laboratory component was determined using the covariance of allele frequency change between the ambient and each treatment group while selection was identified as the covariance within a treatment group minus the laboratory adaptation. The remaining variance was attributed to drift and replicate-specific response to selection.

After identifying the selection and laboratory components of allele frequency change, the remaining variance represents nonparallel changes across replicates. These nonparallel responses could be due to either drift or unique selection responses between the replicates, which we could not distinguish here. Across all selection regimes, variance due to drift or replicate-specific responses was larger for acidification than warming or OWA (Fig. 3*C*), suggesting that selection had less of an impact on allele frequency change under acidification relative to the other treatments.

Last, we quantified the shared response to selection between OWA, warming, and acidification with and without removing estimated laboratory adaptation effects. We calculated the mean pairwise covariance between each group scaled by the total variance. When laboratory adaptation was not removed, acidification shared a response with both OWA (8.4% CI[7.0, 9.8]) and warming (10.3% CI[8.9, 11.8]) (Fig. 4). However, when laboratory adaptation was removed, acidification shared no response with warming (−0.25% CI[−1.36, 0.87]) and a minimal response with OWA (1.12% CI[0.02, 2.21]). In contrast, the OWA and warming lines shared a large proportion of their allele frequency change both with (37.1% CI[35.9, 38.4]) and without (43.5% CI[42.3, 44.6]) accounting for laboratory adaptation.

There were modest increases in linkage disequilibrium (LD) that scaled with the strength of selection where the OWA lines showed the largest increase relative to the founding population (*SI Appendix*, Fig. S5), suggesting a lack of hard selective sweeps acting on single haplotypes. Note that linkage estimates were sensitive to parameters of the method LDx (35) but relative differences between the treatments were consistent regardless of model settings; care should be taken when interpreting the estimates of linkage from this method. There was no link between the response to selection and genome-wide genetic diversity (Tajima's π), though diversity fell by 7 to 14% across all treatment groups from the starting diversity of the founding population replicates (0.0148 ± 0.0004; *SI Appendix*, Fig. S6; Wilcoxon signed-rank test, $P < 0.0001$). This drop was greatest in the acidification line (14% decrease; 0.0127 ± 0.0004), followed by ambient (10% decrease; 0.0133 ± 0.0004) and warming (10% decrease; 0.0133 ± 0.0002), and finally OWA (7% decrease; 0.0138 ± 0.0004). These drops in diversity were not significantly different between treatments, with the exception of the acidification line, which decreased more than other treatments ($P < 0.001$). The relatively small drop in diversity for OWA and warming lines was likely due to the high minor allele frequencies of adaptive alleles; candidate SNPs were at higher minor allele frequency than the genome-wide distribution (*SI Appendix*, Fig. S7). Thus, shifts in frequency of these more common variants could occur without purging variation from the populations.

Discussion

The broad distribution, large population size, and variable coastal habitats inhabited by *A. tonsa* should, in theory, lead to the presence of adaptive genetic variation for evolution in response to stressors under global change. Our results showed that adaptation to warming and OWA conditions was dominated by selection (Fig. 3), indicating the presence of standing genetic variation for rapid adaptation. In contrast, the contribution of selection to allele frequency change under acidification alone was much smaller and the shared response to selection between acidification and OWA was low (Figs. 2 and 4). Combined with the high overlap in the selective response between OWA and warming, this indicated that warming had a much stronger contribution to the OWA selection response than acidification. Despite this, the combined effects of warming and acidification were synergistic, leading to a unique response to selection under OWA conditions relative to the single stressors (Figs. 2 and 4). Thus, adaptive pathways to a single stressor are not indicative of adaptation pathways in a multiple-stressor environment.

The dominance of warming relative to acidification in driving adaptation in OWA conditions is in agreement with work in other systems showing that dominant selective pressures drive the majority of evolutionary change under multistressor adaptation. For example, Brennan et al. (36) found that a few selective pressures predominantly drove adaptive responses of the single-cell algae *Chlamydomonas reinhardtii*, even when up to seven simultaneous stressors were used. However, their work also showed that selection was stronger under multistressor conditions. Our results support these findings where the majority of the selective response under OWA conditions was driven by warming. Nevertheless, the combined effects of warming and acidification were synergistic, leading to a unique response to

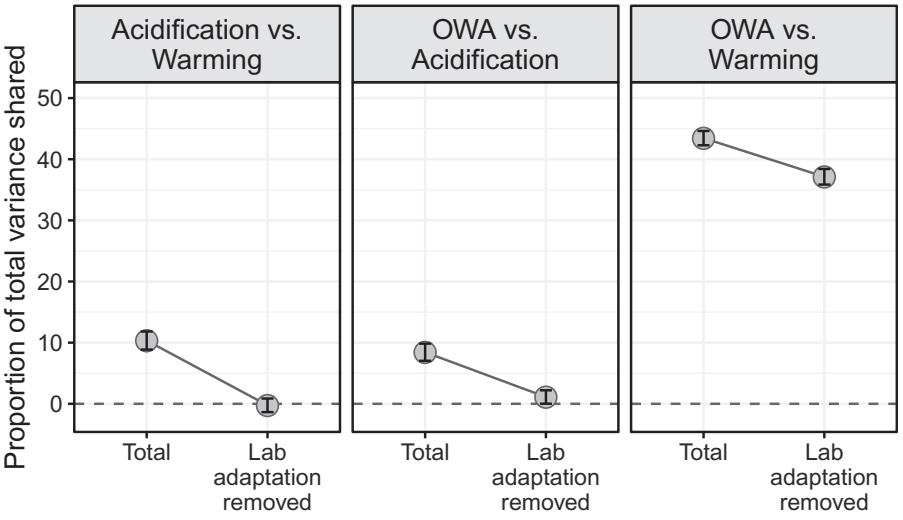

Fig. 4. Shared variance in response to selection between treatments with and without accounting for laboratory adaptation. Error bars represent 95% bootstrapped CIs.

selection under OWA conditions relative to the single stressors (Figs. 2 and 4). Previous work in marine (37) and terrestrial systems (38) has shown that phenotypic responses to multiple stressors are commonly synergistic, including under warming and acidification (39). Our results further demonstrate that the mechanisms of adaptation to a single stressor are not indicative of the mechanisms underlying adaptation to multiple stressors.

In accordance with the synergistic response under multiple-stressor conditions, we observed the largest unique response to selection in the OWA treatment (Fig. 2). Our previous work has shown that hatching success was the primary trait under selection in this experiment and the recovery of this trait was predominantly responsible for adaptation of OWA animals (33). As such, one might predict that processes related to development or hatching would be overrepresented in the OWA adaptive loci. Indeed, we observed GO enrichment of OWA unique adaptive SNPs for mechanisms related to development and morphogenesis (*SI Appendix*, Table S2), including in the adenosine triphosphate (ATP)–dependent helicase DDX39 gene, which regulates cellular differentiation and proliferation and is involved in development and morphogenesis in frogs (*Xenopus*) and fish (*Danio rerio*) (40, 41). While selection on developmental processes is an interesting candidate mechanism of adaptation, more work is needed to verify this hypothesis.

The shared response to selection between OWA and warming indicated that warming was the major driver of OWA adaptation (Figs. 2 and 4). OWA and warming animals developed 22 to 24% faster than ambient and acidification animals, though developmental rates within treatments did not change across the experiment (33). Increased developmental rates may result in selection for physiological processes related to increased metabolic and growth rates, consistent with the observed GO enrichment in shared adaptive loci between OWA and warming (*SI Appendix*, Table S2). Increased temperature can also reduce the energy available for critical functions such as reproduction (42). Similarly, variation in mitochondrial function plays a role in thermal tolerance as high temperatures can inhibit ATP synthesis (43), as has been demonstrated in copepods previously (44). Two mitochondrial genes fundamental to the electron transport chain, NADH dehydrogenase 1 alpha and beta, were identified as under selection and may play a role in metabolic responses to temperature (*SI Appendix*, Fig. S8), though we did not directly quantify metabolic efficiency in this study. Finally, heat shock proteins can drive heat tolerance (45–47). There was evidence of significant enrichment for mechanisms related to protein stabilization (*SI Appendix*, Table S2), including *DNAJA3*, DnaJ heat shock protein family (Hsp40) member A3 (*SI Appendix*, Fig. S8), an inducible heat shock protein that is responsive to temperature and general stress conditions (48). While we hypothesize that these candidates may be involved in adaptation, direct physiological evidence focused on developmental processes, metabolic functioning, and protein stabilization, among other functions, is needed to understand the mechanisms driving adaptation to OWA and warming conditions.

In contrast to OWA and warming, acidification showed a relatively limited response to selection (Figs. 2 and 4). One possible explanation is that acidification alone is not physiologically challenging for *A. tonsa*. Previous work on *A. tonsa* has demonstrated that acidification can be tolerated through phenotypic plasticity (24), and our past study has shown that selection is minimal in the acidification treatment (33). Alternatively, in this experimental design, it is not possible to disentangle the signals of drift from nonparallel responses to selection between replicates (49, 50). However, there is no obvious reason why nonparallel responses to selection would be more common under acidification as compared with the other selection regimes. Finally, it is possible that the majority of the adaptive signal under acidification is simply a general stress response and was shared with all other selection lines (Fig. 2), as discussed below.

There was a consistent response to selection between the ambient line and all treatment groups, suggesting a shared adaptive response to laboratory rearing conditions. However, the contribution of this shared response to allele frequency change was much smaller than selection and drift components (Fig. 3*C*) and treatment-specific responses to selection were dominant for warming and OWA. This shared signal of adaptation may be due to consistent laboratory conditions that favor specific phenotypes across all treatments, such as the density of cultures, ad libitum food, and constant salinity, temperature, and pH. However, there was no shift in fitness in the ambient lines from F0 to F25, suggesting that the target of selection was an unmeasured trait or physiological process (33), and there was little functional enrichment among these laboratory adaptation loci (*SI Appendix*, Table S2). Though the functional consequence is unknown, it was important to account for the presence of potential laboratory adaptation when disentangling the shared and unique responses to selection across groups. When laboratory effects were not removed, the overlap in candidate SNPs (Fig. 2) and the shared response to selection between treatments (Fig. 4) were substantially higher. This was particularly true for acidification where there was limited unique response to selection. Our extension of Buffalo and Coop's covariance methods (14) revealed that all of the shared variance between acidification and warming as well as the majority between acidification and OWA were due to a shared adaptation to laboratory conditions (Fig. 3). These results demonstrate the importance of accounting for laboratory effects and, through both the covariance and candidate SNP analyses, serve as a starting point for others to account for these effects in future work.

The enrichment of the candidate SNPs in coding regions for OWA and warming indicates that protein-coding variation, rather than regulatory variation, may be the dominant target of selection and the main mechanism of adaptation under these constant selection regimes. Our previous work with the *A. tonsa* system has shown that gene expression rapidly evolved in response to OWA selection and there was no link between the genes that changed expression and allele frequency changes (51). Despite this, there were signals of selection in regulators of gene expression such as transcription factors (51), suggesting that coding changes for transregulatory factors may be driving changes in expression. However, we cannot directly test for the effects of transregulatory changes on expression in this experiment as we do not have gene expression from these replicates to link expression to genotype. Furthermore, we have limited power to detect selection in regulatory regions due to sequencing of only a small upstream region of each gene. Thus, our coverage of regulatory variation and our power to detect selection in these regions are limited. Whole-genome sequencing, rather than capture sequencing, would be needed to more thoroughly explore the relative roles of protein coding versus regulatory variation in rapid evolution, though in the present study capture sequencing was necessary given the genome size of *A. tonsa*, 2.5 Gb (52). Thus, while the dominant signals of selection were found in coding regions, the evolution of regulatory elements influencing expression patterns is likely involved in the adaptation process.

Under a hard sweep scenario, we would expect pronounced reductions in genetic diversity that scale with the strength of selection (53). The lack of connection between the strength

and response to selection with genetic diversity coupled with the intermediate frequencies of selected alleles indicates that selection proceeded via soft, polygenic sweeps (*SI Appendix*, Figs. S6 and S7). Similarly, while the increase in LD scaled according to the intensity of selection and was highest in OWA, the difference between treatments was negligible (*SI Appendix*, Fig. S5). From a quantitative genetic perspective, polygenic selection is likely to result in relatively small allele frequency shifts at many loci (12). This is supported by the broad allele frequency responses coupled with few loci with large shifts (*SI Appendix*, Fig. S2). Variants at higher frequency are more likely to fix during adaptation and thus may play an important role during the adaptation process (54, 55). These high-frequency loci are likely maintained by balancing selection (56) perhaps due to naturally fluctuating environmental conditions in typical coastal habitats inhabited by *A. tonsa* (57, 58) and rapid adaptation commonly targets alleles at intermediate frequency (49, 59–61). In particular, Stern and Lee (62) found that balancing selection maintained standing genetic variation that was selected upon during the rapid freshwater adaptation of the invasive copepod *Eurytemora affinis*. It is likely that a similar balancing selection mechanism is involved in maintaining the adaptive genetic variation we observe here. Alternatively, we may have missed signals of hard sweeps with our capture sequencing approach.

Covariance-based analyses represent an advance in our ability to identify selection in temporal datasets that are adapting via polygenic selection (14, 15). However, there are some important limitations to this approach. First, both covariance and frequency change methods, such as CMH, identify targets of selection that are consistent across the replicates of each treatment. This assumption does not always hold as polygenic traits can be genetically redundant and adaptation can proceed through unique pathways (63, 64). As a result, our identification of candidates and the proportion of allele frequency change due to selection are prone to false negatives; there are likely adaptive loci that are unique targets of selection in only a subset of replicates. Thus, our selection component of allele frequency change is a conservative lower bound. The unique targets of selection are impossible to distinguish from drift with the four replicates we used here; an experimental design with much higher replication would be necessary to distinguish these mechanisms (49). Therefore, in the results presented here, the drift and replicate-specific response categories are conflated. Conversely, linked selection and LD can lead to false positives in the candidate gene approach, inflating the number of candidates (65) and the estimates of shared response to selection were higher using the CMH method as compared with cvtk (Figs. 2 and 4). The differences between the two methods is likely due to the fact that cvtk quantifies the contribution of shared covariance to the total variance of allele frequency change in windows without requiring a significance threshold, making it powerful in detecting subtle allele frequency change (14). In contrast, the CMH tests each locus individually and may overestimate the number of candidate SNPs in some cases; our simulations assumed independence between loci, which was a simplification as physical linkage extends ∼200 bp (*SI Appendix*, Fig. S5). Thus, it is likely that the CMH analysis overestimates the effects of selection due to linkage while missing polygenic signals of adaptation.

Our full-factorial evolution experiment demonstrated the complexity of predicting responses to global change conditions when multiple environmental parameters are simultaneously changing. We show that selection weakly affected allele frequencies across the genome for acidification alone (Figs. 2 and 4) which corresponds to the previously observed limited impact on fitness (33). However, when coupled with warming to create OWA conditions, the response to selection was nonadditive and synergistic; only 1 and 37% of the total variation in allele frequency changes in OWA lines were shared with acidification or warming, respectively (Fig. 4). Similarly, of the response to selection in OWA conditions, 47% was not shared with either the acidification or warming selection regimes. These results suggest that a large proportion of the OWA response to selection is unique from either individual component of the selection regime. This has consequences for our ability to predict targets of selection and resilience from genomic data in natural populations. Even relatively benign stressors, such as pH decreases for copepods, can have important impacts when paired with other abiotic changes. As such, predicting resilience or adaptive potential becomes more difficult as the number of changes to the environment increases. Conversely, the shared response to selection and common functional targets between OWA and the single stressors suggests that, functionally, many of the responses are related. Finally, the large, shared signal of selection between OWA and warming suggests that adaptive potential for increased temperature will be a dominant component enabling resilience as the climate continues to change.

Methods

Selection Experiment. The details of the selection experiment have been reported previously in Dam et al. (33). This experiment was conducted with four replicates per treatment designed to simulate future ocean conditions that were warmer and more acidic with the following target environments: 1) ambient (18 °C, 400 μatm CO_2, pH ∼8.2); 2) acidification (18 °C, 2,000 μatm CO_2, pH ∼7.5); 3) warming (22 °C, 400 μatm CO_2, pH ∼8.2); and 4) OWA (22 °C, 2,000 μatm CO_2, pH ∼7.5). These levels were chosen as ambient conditions represent current conditions in the native habitat, while elevated CO_2 and temperature align with predicted future conditions in the years 2100 to 2300 (66, 67). Four replicates is generally considered suitable to achieve good power in E&R experiments (68). Temperature treatments were achieved using four incubators, two for 22 °C and the other two for 18 °C, while elevated CO_2 was controlled by continuously mixing CO_2 directly into the bottom of each replicate. Ambient CO_2 conditions were achieved by mixing CO_2-stripped air into each culture. Dissolved oxygen was >8 mg·L^{-1} for all cultures.

Adult *A. tonsa* (n = 1,000) were collected in June of 2016 from Esker Point Beach, Groton, CT, USA (41.320725°N, 72.001643°W). We allowed the field-collected animals to acclimate to the laboratory conditions for three generations before initiating experimental replicates. To initiate temperature treatments, eight replicate cultures were each started with 160 adult females and 80 adult males. Within a single generation, four of these eight cultures had temperature increased by 1 °C·d^{-1} while the others remained at ambient temperature. After temperature acclimation, which occurred over 4 d, adults were allowed to lay eggs, producing an average of 7,173 eggs per replicate. The warm treatment replicates (four of each for OWA and warming) were seeded by the warm acclimation animals (average of 3,586 per replicate) and the ambient temperature treatments by the ambient animals. Cultures were fed equal concentrations of phytoplankters *Tetraselmis* sp., *Rhodomonas* sp., and *Thalassiosira weissflogii* every 2 to 3 d at food-replete condition (≥800 μg carbon·L^{-1}), following established protocols (69). All cultures were held in 10-L square containers (Cambro) with aeration at a salinity of 32.75 (CI[32.4, 33.46]) Practical Salinity Units and 12 h light, 12 h dark. Cultures were reared for 25, nonoverlapping, generations with population sizes >3,000 per replicate. Samples for genomic analysis were collected from each replicate from the ambient treatment at F0 to represent the starting population allele frequencies and from each of the selection regimes, including ambient, at F25.

Genome Annotation. We based genomic analysis on the publicly available, yet unannotated, *A. tonsa* genome (52). We followed the GAWN annotation pipeline (https://github.com/enormandeau/gawn) to complete the annotation of the existing assembly. GAWN takes an evidence-based approach to assembly, using an assembled transcriptome as the evidence for gene models; we leveraged the high-quality transcriptome from Jørgensen et al. (52) for this purpose. Briefly, this method uses GMAP (70) to align the transcriptome to the genome, transdecoder (71) to determine open reading frames, and blastx (72) to annotate predicted genes.

SNP Identification. Capture probes were designed to target regulatory and coding regions across the genome. Regulatory probes were located within 1,000 bp upstream of transcription start sites and coding probes were located in exons; both regulatory and exonic probes were chosen to maximize capture quality. This process resulted in 32,413 probes (21,311 exonic, 11,102 regulatory). DNA library preparation and sequencing were conducted by Rapid Genomics on a HiSeq 4000 with 150-bp paired-end reads.

Raw reads were trimmed for quality and adapter contamination with Trimmomatic v. 0.36 (73) and mapped to the *A. tonsa* reference genome (52) with BWA-MEM (74). Raw data are deposited in NCBI: BioProject no. PRJNA590963. Variants were called using VarScan 2 (75) with a minimum variant frequency of 0.01, *P* value of 0.1, minimum alternate reads 2, and minimum coverage of 30×, resulting in 10,368,816 sites. Sites were then filtered for coverage >40× in all samples, minor allele frequency >0.01 in at least four samples (i.e., one treatment), including only biallelic sites, and excluding sites with depth per sample above the 97.5% quantile (912×) to control for mismapping; changing the 97.5% threshold to 95% did not alter overall results. This filtering resulted in a final set of 394,667 variant sites.

Characterizing Genetic Variation. We summarized genome-wide variation in allele frequencies between all samples using PCA with the prcomp function in R (76). To understand the demographic impacts of the selection regimes, we estimated levels of LD and genetic diversity (π) for all replicates. LD was estimated using LDx, a Pool-Seq method that uses haplotype information from single read pairs to estimate linkage between pairs of SNPs over short distances (35). We estimate the decay of LD by regression of the log of physical distance with LD between base pairs; to estimate the slope and intercept of each treatment, we include replicate as a random effect with the R package lme (77).

Genetic diversity was estimated using PoPoolation (78). We estimated π in 100-bp sliding windows with a 100-bp step size, resulting in 1,940 100-bp windows in 987 unique scaffolds across the genome that were present across all samples. Each window required a minimum coverage of 15×, maximum coverage of 1,000× (to avoid mapping errors), and at least 0.5 of the window meeting these thresholds. To take into account the independent replicates within each treatment, we used pairwise Wilcoxon rank-sum tests with a Holm correction for multiple testing. All statistics were performed in R (76).

Clade Assignment. *A. tonsa*, while broadly distributed, is made up of mitochondrial lineages that likely represent cryptic species (79–81), at least two of which are reproductively isolated (82). We reconstructed mitochondrial cytochrome oxidase subunit I (COI) haplotypes present in the starting and F25 cultures to ensure adaptation signals were not simply shifts in cryptic species composition of the cultures. Raw fastq files were aligned to COI sequences from Figueroa et al. (79), calling variants in the same manner as the full dataset. The distribution of allele frequencies of these variants was bimodal, with nearly all variants close to fixation (*SI Appendix*, Fig. S9). We generated consensus sequences for the major and minor variant for each sample and generated phylogenetic trees using MrBayes (83), including samples from Figueroa et al. (79) and following their analysis. The mitochondrial lineage of the animals in this experiment was clade X from Figueroa et al. (79) (*SI Appendix*, Fig. S10); results were validated by Sanger sequencing COI of individual copepods from these same cultures at approximately generation 100. Thus, any differential signals of adaptation between experimental conditions were not due to the presence of cryptic species in the samples but rather selection within each condition acting on the same lineage's genetic variation. See *SI Appendix*, *Materials* for more details.

Estimates of Allele Frequency Change within and between Treatments. Disentangling the extent to which the variance in allele frequency change within and between treatments is due to selection (rather than random genetic drift) is difficult due to the subtle changes that can occur during polygenic adaptation. To overcome this limitation, we used cvtk (https://github.com/vsbuffalo/cvtkpy) (14, 15), which uses the replication within treatments to calculate covariance between samples and partition the variance in allele frequency change from F0 to F25 into its various components. Consistent temporal allele frequency changes within a treatment are considered due to selection. Nonparallel shifts are attributed to drift or replicate-specific responses to selection, which we cannot tell apart with these data; more dense temporal sampling or randomized matings to generate null drift expectations (13) could help distinguish these responses (14, 49). Further, this framework can be used to assess the convergent correlation between different treatments to quantify the degree to which different selection regimes drive allele frequency change in common genomic regions. Finally, we extended cvtk to incorporate signals of laboratory adaptation. Because the ambient control should only be selected for laboratory conditions, any covariance between this control and the selection lines indicates adaptation to the laboratory environment. We calculated the covariance of allele frequency change from F0 to F25 in 10,000-bp windows for each replicate and used these estimates to calculate the proportion of the change of allele frequency due to selection, drift or replicate-specific responses, and laboratory adaptation; results hold when window size is changed to 1,000 bp. Uncertainty was determined with bootstrap resampling of windows, and the variance in sequencing depth and the number of diploids sequenced was accounted for in these methods. See *SI Appendix*, *Materials* for a detailed discussion of these methods.

We determined specific loci evolving due to selection by simulating the expected drift over 25 generations using the Pool-Seq package in R (84) and following Barghi et al. (64). Using the starting allele frequencies at F0, we mirrored our experimental design and simulated allele frequency trajectories for four replicates across 25 generations with no selection under a Wright–Fisher model. We used the Pool-Seq R package (84, 85) to estimate the mean effective population size as 414 across all replicates, and simulated neutral allele frequency changes using this effective population size and a census size of 3,000. We added the same variance as our sampling scheme by estimating allele frequencies from a sample size of 50 individuals and a simulated sequencing depth of 167 at F0 and 106 at F25, matching the observed depth. This simulation was repeated 500 times and, for each replicate, CMH tests in PoPoolation2 (86) were used to generate a null distribution of neutral allele frequency change. Empirical *P* values were calculated from this simulated distribution using empPvals in the qvalue R package (87). Candidate adaptive loci were sites with empirical *P* values less than 0.01. Significance of overlap between sets of candidate SNPs between treatments was calculated using SuperExactTest in R (88).

Functional enrichment was tested using topGO v. 2.36.0 (89, 90) with the weight01 method with terms that had at least five annotated genes. The background gene set was defined as all genes with SNPs in or near them in these data (i.e., all that could be identified in our data). We considered a gene significant if at least one SNP that was annotated to that gene passed the null threshold for selection. We used GOSemSim (91) with Wang's method in R to calculate the similarity between terms with P values < 0.05 and converted this similarity matrix to a dissimilarity matrix for hierarchical clustering and plotting using ggdendro in R (92).

Data, Materials, and Software Availability. Sequence data reported in this article have been deposited in the National Center for Biotechnology Information (NCBI) (BioProject no. PRJNA590963) (93). Tables S1 and S2 can be found in the *SI Appendix* and on Zenodo, https://doi.org/10.5281/zenodo.5093796 (94). Code to run all analyses can be found on Zenodo, https://doi.org/10.5281/zenodo.6979583 (95).

ACKNOWLEDGMENTS. This work was funded by NSF grants (to M.H.P. [OCE 1559075; IOS 1943316] and H.G.D., H.B., and M.F. [OCE 1559180]), as well as a Connecticut Sea Grant (R/LR-25; awarded to H.G.D., M.F., and H.B.). We thank Jon Puritz for helpful feedback on this manuscript.

Author affiliations: [a]Department of Biology, University of Vermont, Burlington, VT 05405; [b]Marine Evolutionary Ecology, GEOMAR Helmholtz Centre for Ocean Research Kiel, Kiel, 24105, Germany; [c]Faculty of Mathematics and Natural Sciences, Christian-Albrechts University of Kiel, Kiel, 24118, Germany; [d]Department of Marine Sciences, University of Connecticut, Groton, CT 06340; [e]Department of Ecology and Evolutionary Biology, University of Connecticut, Groton, CT 06340; and [f]Institute for Ecology and Evolution, University of Oregon, Eugene, OR 97403

1. R. D. H. Barrett, D. Schluter, Adaptation from standing genetic variation. *Trends Ecol. Evol.* **23**, 38–44 (2008).
2. H. C. Bumpus, *The Elimination of the Unfit as Illustrated by the Introduced Sparrow*, Passer domesticus *(A Fourth Contribution to the Study of Variation)* (Gin, 1899).
3. C. M. Donihue *et al.*, Hurricane-induced selection on the morphology of an island lizard. *Nature* **560**, 88–91 (2018).
4. P. De Wit, L. Rogers-Bennett, R. M. Kudela, S. R. Palumbi, Forensic genomics as a novel tool for identifying the causes of mass mortality events. *Nat. Commun.* **5**, 3652 (2014).
5. S. C. Campbell-Staton *et al.*, Winter storms drive rapid phenotypic, regulatory, and genomic shifts in the green anole lizard. *Science* **357**, 495–498 (2017).
6. F. Rodríguez-Trelles, R. Tarrío, M. Santos, Genome-wide evolutionary response to a heat wave in *Drosophila*. *Biol. Lett.* **9**, 20130228 (2013).
7. T. L. Turner, A. D. Stewart, A. T. Fields, W. R. Rice, A. M. Tarone, Population-based resequencing of experimentally evolved populations reveals the genetic basis of body size variation in *Drosophila melanogaster*. *PLoS Genet.* **7**, e1001336 (2011).
8. C. Schlötterer, R. Kofler, E. Versace, R. Tobler, S. U. Franssen, Combining experimental evolution with next-generation sequencing: A powerful tool to study adaptation from standing genetic variation. *Heredity* **114**, 431–440 (2015).
9. C. Vlachos *et al.*, Benchmarking software tools for detecting and quantifying selection in evolve and resequencing studies. *Genome Biol.* **20**, 169 (2019).
10. A.-M. Waldvogel *et al.*, Evolutionary genomics can improve prediction of species' responses to climate change. *Evol. Lett.* **4**, 4–18 (2020).
11. K. E. Kemper, S. J. Saxton, S. Bolormaa, B. J. Hayes, M. E. Goddard, Selection for complex traits leaves little or no classic signatures of selection. *BMC Genomics* **15**, 246 (2014).
12. J. K. Pritchard, J. K. Pickrell, G. Coop, The genetics of human adaptation: Hard sweeps, soft sweeps, and polygenic adaptation. *Curr. Biol.* **20**, R208–R215 (2010).
13. J. P. Castro *et al.*, An integrative genomic analysis of the Longshanks selection experiment for longer limbs in mice. *eLife* **8**, e42014 (2019).
14. V. Buffalo, G. Coop, Estimating the genome-wide contribution of selection to temporal allele frequency change. *Proc. Natl. Acad. Sci. U.S.A.* **117**, 20672–20680 (2020).
15. V. Buffalo, G. Coop, The linked selection signature of rapid adaptation in temporal genomic data. *Genetics* **213**, 1007–1045 (2019).
16. S. C. Doney, V. J. Fabry, R. A. Feely, J. A. Kleypas, Ocean acidification: The other CO_2 problem. *Annu. Rev. Mar. Sci.* **1**, 169–192 (2009).
17. C. Pelejero, E. Calvo, O. Hoegh-Guldberg, Paleo-perspectives on ocean acidification. *Trends Ecol. Evol.* **25**, 332–344 (2010).
18. K. Banse, Zooplankton: Pivotal role in the control of ocean production: I. Biomass and production. *ICES J. Mar. Sci.* **52**, 265–277 (1995).
19. H. G. Dam, X. Zhang, M. Butler, M. R. Roman, Mesozooplankton grazing and metabolism at the equator in the central Pacific: Implications for carbon and nitrogen fluxes. *Deep Sea Res. 2 Top. Stud. Oceanogr.* **42**, 735–756 (1995).
20. C. Möllmann, B. Müller-Karulis, G. Kornilovs, M. A. St John, Effects of climate and overfishing on zooplankton dynamics and ecosystem structure: Regime shifts, trophic cascade, and feedback loops in a simple ecosystem. *ICES J. Mar. Sci.* **65**, 302–310 (2008).
21. P. Thor, S. Dupont, Transgenerational effects alleviate severe fecundity loss during ocean acidification in a ubiquitous planktonic copepod. *Glob. Change Biol.* **21**, 2261–2271 (2015).
22. M. Sasaki, H. G. Dam, Global patterns in copepod thermal tolerance. *J. Plankton Res.* **43**, 598–609 (2021).
23. M. W. Kelly, E. Sanford, R. K. Grosberg, Limited potential for adaptation to climate change in a broadly distributed marine crustacean. *Proc. Biol. Sci.* **279**, 349–356 (2012).
24. J. A. F. Langer *et al.*, Acclimation and adaptation of the coastal calanoid copepod *Acartia tonsa* to ocean acidification: A long-term laboratory investigation. *Mar. Ecol. Prog. Ser.* **619**, 35–51 (2019).
25. P. De Wit, S. Dupont, P. Thor, Selection on oxidative phosphorylation and ribosomal structure as a multigenerational response to ocean acidification in the common copepod *Pseudocalanus acuspes*. *Evol. Appl.* **9**, 1112–1123 (2015).
26. C. E. Lee, J. L. Remfert, Y.-M. Chang, Response to selection and evolvability of invasive populations. *Genetica* **129**, 179–192 (2007).
27. C. E. Lee, M. Kiergaard, G. W. Gelembiuk, B. D. Eads, M. Posavi, Pumping ions: Rapid parallel evolution of ionic regulation following habitat invasions. *Evolution* **65**, 2229–2244 (2011).
28. M. W. Kelly, M. S. Pankey, M. B. DeBiasse, D. C. Plachetzki, Adaptation to heat stress reduces phenotypic and transcriptional plasticity in a marine copepod. *Funct. Ecol.* **31**, 398–406 (2017).
29. J. S. Griffiths, Y. Kawji, M. W. Kelly, An experimental test of adaptive introgression in locally adapted populations of splash pool copepods. *Mol. Biol. Evol.* **38**, 1306–1316 (2021).
30. P. W. Boyd *et al.*, Experimental strategies to assess the biological ramifications of multiple drivers of global ocean change–A review. *Glob. Change Biol.* **24**, 2239–2261 (2018).
31. A. R. Gunderson, E. J. Armstrong, J. H. Stillman, Multiple stressors in a changing world: The need for an improved perspective on physiological responses to the dynamic marine environment. *Annu. Rev. Mar. Sci.* **8**, 357–378 (2016).
32. J. T. Turner, "The feeding ecology of some zooplankters that are important prey items of larval fish" (National Oceanic and Atmospheric Administration Tech. Rep. National Marine Fisheries Service 7, 1984).
33. H. G. Dam *et al.*, Rapid, but limited, zooplankton adaptation to simultaneous warming and acidification. *Nat. Clim. Chang.* **11**, 780–786 (2021).
34. M. W. Kelly, J. S. Griffiths, Selection experiments in the sea: What can experimental evolution tell us about how marine life will respond to climate change? *Biol. Bull.* **241**, 30–42 (2021).
35. A. F. Feder, D. A. Petrov, A. O. Bergland, LDx: Estimation of linkage disequilibrium from high-throughput pooled resequencing data. *PLoS One* **7**, e48588 (2012).
36. G. L. Brennan, N. Colegrave, S. Collins, Evolutionary consequences of multidriver environmental change in an aquatic primary producer. *Proc. Natl. Acad. Sci. U.S.A.* **114**, 9930–9935 (2017).
37. M. Seifert, B. Rost, S. Trimborn, J. Hauck, Meta-analysis of multiple driver effects on marine phytoplankton highlights modulating role of pCO_2. *Glob. Change Biol.* **26**, 6787–6804 (2020).
38. J. A. Orr, P. Luijckx, J.-F. Arnoldi, A. L. Jackson, J. J. Piggott, Rapid evolution generates synergism between multiple stressors: Linking theory and an evolution experiment. *Glob. Change Biol.* **28**, 1740–1752 (2022).
39. B. P. Harvey, D. Gwynn-Jones, P. J. Moore, Meta-analysis reveals complex marine biological responses to the interactive effects of ocean acidification and warming. *Ecol. Evol.* **3**, 1016–1030 (2013).
40. J. M. Wilson *et al.*, RNA helicase Ddx39 is expressed in the developing central nervous system, limb, otic vesicle, branchial arches and facial mesenchyme of *Xenopus laevis*. *Gene Expr. Patterns* **10**, 44–52 (2010).
41. L. Zhang, Y. Yang, B. Li, I. C. Scott, X. Lou, The DEAD-box RNA helicase Ddx39ab is essential for myocyte and lens development in zebrafish. *Development* **145**, dev161018 (2018).
42. P. M. Schulte, The effects of temperature on aerobic metabolism: Towards a mechanistic understanding of the responses of ectotherms to a changing environment. *J. Exp. Biol.* **218**, 1856–1866 (2015).
43. D. J. Chung, P. M. Schulte, Mitochondria and the thermal limits of ectotherms. *J. Exp. Biol.* **223**, jeb227801 (2020).
44. A. E. Harada, T. M. Healy, R. S. Burton, Variation in thermal tolerance and its relationship to mitochondrial function across populations of *Tigriopus californicus*. *Front. Physiol.* **10**, 213 (2019).
45. M. E. Feder, G. E. Hofmann, Heat-shock proteins, molecular chaperones, and the stress response: Evolutionary and ecological physiology. *Annu. Rev. Physiol.* **61**, 243–282 (1999).
46. J. G. Sørensen, Application of heat shock protein expression for detecting natural adaptation and exposure to stress in natural populations. *Curr. Zool.* **56**, 703–713 (2010).
47. S. Tangwancharoen, G. W. Moy, R. S. Burton, Multiple modes of adaptation: Regulatory and structural evolution in a small heat shock protein gene. *Mol. Biol. Evol.* **35**, 2110–2119 (2018).
48. M. P. Mayer, B. Bukau, Hsp70 chaperones: Cellular functions and molecular mechanism. *Cell. Mol. Life Sci.* **62**, 670–684 (2005).
49. N. Barghi *et al.*, Genetic redundancy fuels polygenic adaptation in *Drosophila*. *PLoS Biol.* **17**, e3000128 (2019).
50. N. O. Therkildsen *et al.*, Contrasting genomic shifts underlie parallel phenotypic evolution in response to fishing. *Science* **365**, 487–490 (2019).
51. R. S. Brennan *et al.*, Loss of transcriptional plasticity but sustained adaptive capacity after adaptation to global change conditions in a marine copepod. *Nat. Commun.* **13**, 1147 (2022).
52. T. S. Jørgensen *et al.*, The genome and mRNA transcriptome of the cosmopolitan calanoid copepod *Acartia tonsa* Dana improve the understanding of copepod genome size evolution. *Genome Biol. Evol.* **11**, 1440–1450 (2019).
53. P. S. Pennings, J. Hermisson, Soft sweeps II–Molecular population genetics of adaptation from recurrent mutation or migration. *Mol. Biol. Evol.* **23**, 1076–1084 (2006).
54. P. W. Messer, S. P. Ellner, N. G. Hairston Jr., Can population genetics adapt to rapid evolution? *Trends Genet.* **32**, 408–418 (2016).
55. J. Hermisson, P. S. Pennings, Soft sweeps: Molecular population genetics of adaptation from standing genetic variation. *Genetics* **169**, 2335–2352 (2005).
56. I. Höllinger, P. S. Pennings, J. Hermisson, Polygenic adaptation: From sweeps to subtle frequency shifts. *PLoS Genet.* **15**, e1008035 (2019).
57. S. W. Nixon, S. Granger, B. A. Buckley, M. Lamont, B. Rowell, A one hundred and seventeen year coastal water temperature record from Woods Hole, Massachusetts. *Estuaries* **27**, 397–404 (2004).
58. H. Baumann, E. M. Smith, Quantifying metabolically driven pH and oxygen fluctuations in US nearshore habitats at diel to interannual time scales. *Estuaries Coast.* **41**, 1102–1117 (2018).
59. R. S. Brennan, A. D. Garrett, K. E. Huber, H. Hargarten, M. H. Pespeni, Rare genetic variation and balanced polymorphisms are important for survival in global change conditions. *Proc. Biol. Sci.* **286**, 20190943 (2019).
60. J. K. Kelly, K. A. Hughes, Pervasive linked selection and intermediate-frequency alleles are implicated in an evolve-and-resequencing experiment of *Drosophila simulans*. *Genetics* **211**, 943–961 (2019).
61. F. Mallard, V. Nolte, R. Tobler, M. Kapun, C. Schlötterer, A simple genetic basis of adaptation to a novel thermal environment results in complex metabolic rewiring in *Drosophila*. *Genome Biol.* **19**, 119 (2018).
62. D. B. Stern, C. E. Lee, Evolutionary origins of genomic adaptations in an invasive copepod. *Nat. Ecol. Evol.* **4**, 1084–1094 (2020).
63. Á. J. Láruson, S. Yeaman, K. E. Lotterhos, The importance of genetic redundancy in evolution. *Trends Ecol. Evol.* **35**, 809–822 (2020).
64. N. Barghi, J. Hermisson, C. Schlötterer, Polygenic adaptation: A unifying framework to understand positive selection. *Nat. Rev. Genet.* **21**, 769–781 (2020).
65. R. Tobler *et al.*, Massive habitat-specific genomic response in *D. melanogaster* populations during experimental evolution in hot and cold environments. *Mol. Biol. Evol.* **31**, 364–375 (2014).
66. K. Caldeira, M. E. Wickett, Oceanography: Anthropogenic carbon and ocean pH. *Nature* **425**, 365 (2003).
67. N. L. Bindoff *et al.*, "Changing ocean, marine ecosystems, and dependent communities" in *IPCC Special Report on the Ocean and Cryosphere in a Changing Climate*, H.-O. Pörtner *et al.*, Eds. (Cambridge University Press, 2019), pp. 447–587.
68. R. Kofler, C. Schlötterer, A guide for the design of evolve and resequencing studies. *Mol. Biol. Evol.* **31**, 474–483 (2014).
69. L. R. Feinberg, H. G. Dam, Effects of diet on dimensions, density and sinking rates of fecal pellets of the copepod *Acartia tonsa*. *Mar. Ecol. Prog. Ser.* **175**, 87–96 (1998).
70. T. D. Wu, C. K. Watanabe, GMAP: A genomic mapping and alignment program for mRNA and EST sequences. *Bioinformatics* **21**, 1859–1875 (2005).
71. B. J. Haas *et al.*, De novo transcript sequence reconstruction from RNA-seq using the Trinity platform for reference generation and analysis. *Nat. Protoc.* **8**, 1494–1512 (2013).
72. C. Camacho *et al.*, BLAST+: Architecture and applications. *BMC Bioinformatics* **10**, 421 (2009).
73. A. M. Bolger, M. Lohse, B. Usadel, Trimmomatic: A flexible trimmer for Illumina sequence data. *Bioinformatics* **30**, 2114–2120 (2014).
74. H. Li, Aligning sequence reads, clone sequences and assembly contigs with BWA-MEM. arXiv [Preprint] (2013). https://doi.org/10.48550/arXiv.1303.3997 (Accessed 8 March 2018).
75. D. C. Koboldt *et al.*, VarScan 2: Somatic mutation and copy number alteration discovery in cancer by exome sequencing. *Genome Res.* **22**, 568–576 (2012).
76. R Core Team, R: A Language and Environment for Statistical Computing (R Foundation for Statistical Computing, 2013).
77. D. Bates, M. Mächler, B. Bolker, S. Walker, Fitting linear mixed-effects models using lme4. *J. Stat. Softw.* **67**, 1–48 (2015).
78. R. Kofler *et al.*, PoPoolation: A toolbox for population genetic analysis of next generation sequencing data from pooled individuals. *PLoS One* **6**, e15925 (2011).
79. N. J. Figueroa, D. F. Figueroa, D. Hicks, Phylogeography of *Acartia tonsa* Dana, 1849 (Calanoida: Copepoda) and phylogenetic reconstruction of the genus *Acartia Dana*, 1846. *Mar. Biodivers.* **50**, 23 (2020).
80. G. Chen, M. P. Hare, Cryptic ecological diversification of a planktonic estuarine copepod, *Acartia tonsa*. *Mol. Ecol.* **17**, 1451–1468 (2008).

81. G. Chen, M. P. Hare, Cryptic diversity and comparative phylogeography of the estuarine copepod *Acartia tonsa* on the US Atlantic coast. *Mol. Ecol.* **20**, 2425–2441 (2011).
82. L. V. Plough, C. Fitzgerald, A. Plummer, J. J. Pierson, Reproductive isolation and morphological divergence between cryptic lineages of the copepod *Acartia tonsa* in Chesapeake Bay. *Mar. Ecol. Prog. Ser.* **597**, 99–113 (2018).
83. F. Ronquist *et al.*, MrBayes 3.2: Efficient Bayesian phylogenetic inference and model choice across a large model space. *Syst. Biol.* **61**, 539–542 (2012).
84. T. Taus, A. Futschik, C. Schlötterer, Quantifying selection with Pool-Seq time series data. *Mol. Biol. Evol.* **34**, 3023–3034 (2017).
85. Á. Jónás, T. Taus, C. Kosiol, C. Schlötterer, A. Futschik, Estimating the effective population size from temporal allele frequency changes in experimental evolution. *Genetics* **204**, 723–735 (2016).
86. R. Kofler, R. V. Pandey, C. Schlötterer, PoPoolation2: Identifying differentiation between populations using sequencing of pooled DNA samples (Pool-Seq). *Bioinformatics* **27**, 3435–3436 (2011).
87. J. D. Storey, A. J. Bass, A. Dabney, D. Robinson, qvalue: Q-Value Estimation for False Discovery Rate Control (R Package Version 2.16.0, Bioconductor, 2019).
88. M. Wang, Y. Zhao, B. Zhang, Efficient test and visualization of multi-set intersections. *Sci. Rep.* **5**, 16923 (2015).
89. A. Alexa, J. Rahnenführer, T. Lengauer, Improved scoring of functional groups from gene expression data by decorrelating GO graph structure. *Bioinformatics* **22**, 1600–1607 (2006).
90. A. Alexa, J. Rahnenfuhrer, Gene Set Enrichment Analysis with topGO (Version 2.42.0, Bioconductor, 2019).
91. G. Yu *et al.*, GOSemSim: An R package for measuring semantic similarity among GO terms and gene products. *Bioinformatics* **26**, 976–978 (2010).
92. A. de Vries, B. D. Ripley, ggdendro: Create Dendrograms and Tree Diagrams Using 'ggplot2' (R Package Version 0.1.20, R Foundation for Statistical Computing, 2016).
93. R. S. Brennan *et al.*, Acartia tonsa Raw sequence reads: experimental evolution. NCBI BioProject. https://www.ncbi.nlm.nih.gov/bioproject/?term=PRJNA590963. Deposited 21 November 2019.
94. R. S. Brennan, Acartia tonsa 25 generation experimental evolution. Zenodo. https://zenodo.org/record/6684550. Deposited 1 September 2022.
95. R. S. Brennan, rsbrennan/tonsa_25_gen_ER: Version 1.1.0. Zenodo. https://zenodo.org/record/6979584. Deposited 10 August 2022.